

Overview and loss analysis of III–V single-junction and multi-junction solar cells

Masafumi Yamaguchi^{1,*}, Frank Dimroth², Nicholas J. Ekins-Daukes³, Nobuaki Kojima¹, and Yoshio Ohshita¹

¹ Toyota Technological Institute, Nagoya 468-8511, Japan

² Fraunhofer Institute for Solar Energy Systems ISE, Freiburg 79110, Germany

³ University of New South Wales, Sydney 2052, Australia

Received: 2 June 2022 / Received in final form: 26 July 2022 / Accepted: 29 August 2022

Abstract. The development of high-performance solar cells offers a promising pathway toward achieving high power per unit cost for many applications. Because state-of-the-art efficiencies of single-junction solar cells are approaching the Shockley-Queisser limit, the multi-junction (MJ) solar cells are very attractive for high-efficiency solar cells. This paper reviews progress in III–V compound single-junction and MJ solar cells. In addition, analytical results for efficiency potential and non-radiative recombination and resistance losses in III–V compound single-junction and MJ solar cells are presented for further understanding and decreasing major losses in III–V compound materials and MJ solar cells. GaAs single-junction, III–V 2-junction and III–V 3-junction solar cells are shown to have potential efficiencies of 30%, 37% and 47%, respectively. Although in initial stage of developments, GaAs single-junction and III–V MJ solar cells have shown low ERE values, ERE values have been improved as a result of several technology development such as device structure and material quality developments. In the case of III–V MJ solar cells, improvements in ERE of sub-cells are shown to be necessary for further improvements in efficiencies of MJ solar cells.

Keywords: High-efficiency / single-junction solar cells / multi-junction solar cells / loss analysis

1 Introduction

The development of high-performance solar cells offers a promising pathway toward achieving high power per unit cost for many applications. Because state-of-the-art efficiencies of single-junction solar cells are approaching the Shockley-Queisser limit [1], the multi-junction (MJ) solar cells [2] are very attractive for high-efficiency solar cells as shown in Figure 1. Although the concept of MJ solar cells was first and most successfully implemented using III–V compound materials, there is a need to further improve their conversion efficiency of III–V MJ solar cells and to show guidelines for realizing high-efficiency MJ solar cells composed of other materials like perovskite, II–VI compounds and chalcogenides.

This paper reviews progress in III–V compound single-junction and multi-junction solar cells. In addition, analytical results for efficiency potential and non-radiative recombination and resistance losses in III–V compound single-junction and multi-junction solar cells are presented

for further understanding and decreasing major losses in III–V compound materials and multi-junction solar cells.

2 Overview for III–V single-junction and multi-junction solar cells

Figure 2 summarizes chronological improvements in conversion efficiencies of Si, GaAs, CIGS and perovskite single-junction solar cells and III–V compound multi-junction solar cells under 1-sun operation [3] and future efficiency predictions of those solar cells (original idea by Professor A. Goetzberger et al. [4] and modified by M. Yamaguchi et al. [5]).

The function chosen here (Eq. (1)) is derived from the diode equation:

$$\eta(t) = \eta_L \{1 - \exp[(a_0 - a)/c]\}, \quad (1)$$

where $\eta(t)$ is the time-dependent efficiency, η_L limiting asymptotic maximum efficiency, a_0 is the year for which $\eta(t)$ is zero, a is the calendar year and c is a characteristic development time. Fitting of the curve is done with three

* e-mail: masafumi@toyota-ti.ac.jp

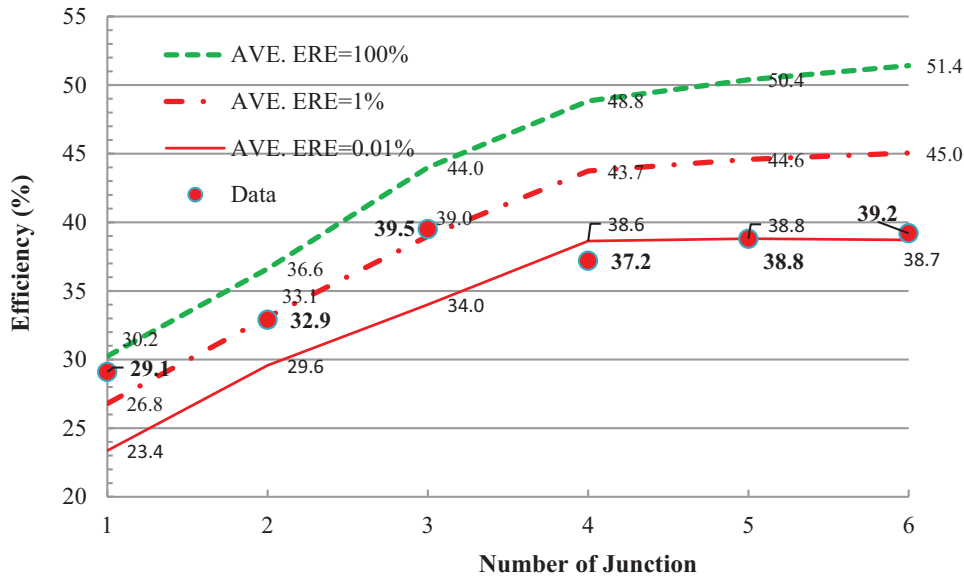


Fig. 1. Calculated efficiencies of III–V compound MJ solar cells under 1-sun condition as a function of the number of junction and average external radiative efficiency (ERE) [2] in comparison with efficiency data (best laboratory efficiencies [3]). (Reproduced with permission from Ref. [2]. Updated).

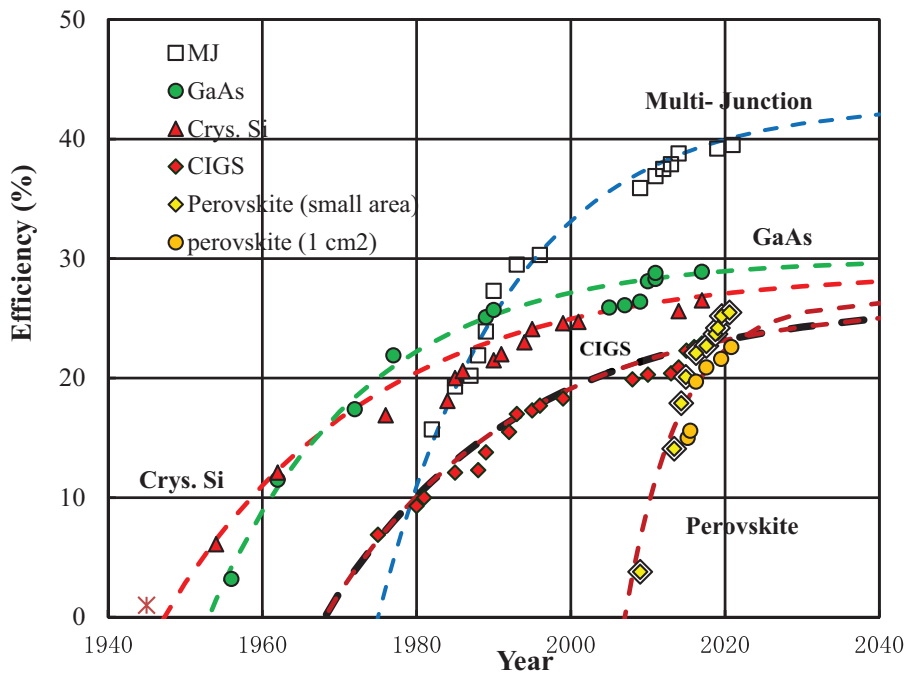


Fig. 2. Chronological efficiency improvements of crystalline Si, GaAs, CIGS, and perovskite single-junction solar cells and III–V compound multi-junction (MJ) solar cells under 1-sun condition.

parameters which are given in Table 1. For example, 43% for η_L , 17 for a_0 and 1975 for c were used in the case of III–V compound multi-junction solar cells. The function can be fitted relatively well to the past development of best laboratory efficiencies of various solar cells under 1-sun condition.

3 Analytical procedure for estimating efficiency potential of various solar cells

One of the problems to attain the higher efficiency MJ and Si tandem solar cells is to reduce non-radiative recombination

Table 1. Fitting parameters for different technologies.

Solar cell	η_L	c	a_0
Single-crystal Si	29	26.8	1947.2
GaAs	30	20	1953
CIGSe	26.5	25	1968
Perovskite (1 cm ²)	26.5	7	2007
III–V multi-junction	43	17	1975

loss. The open-circuit voltage V_{oc} drop compared to bandgap energy ($Eg/q - V_{oc}$) is dependent upon non-radiative voltage loss ($V_{oc,nrad}$) that is expressed by external radiative efficiency (ERE). Open-circuit voltage is expressed by [6–10]

$$V_{oc} = V_{oc,rad} + (kT/q)\ln(\text{ERE}), \quad (2)$$

where the second term on the right-hand side of equation (2) is denoted as $V_{oc,nrad}$ because it is associated to the voltage-loss due to non-radiative recombination and $V_{oc,rad}$ is radiative open-circuit voltage and is given by [6–10]

$$V_{oc,rad} = (kT/q)\ln(J_L(V_{oc,rad})/J_{0,rad} + 1), \quad (3)$$

where $J_L(V_{oc,rad})$ is photo-current at open-circuit in the case of only radiative recombination and $J_{0,rad}$ is saturation current density in the case of only radiative recombination. 0.28 V [8–10] for III–V compounds and perovskite, and 0.26 V [8–10] for Si solar cells were used as $\Delta V_{oc,rad} (= Eg/q - V_{oc,rad})$ in this study. In the case of multi-junction tandem solar cells, we define average ERE (ERE_{ave}) by using average V_{oc} loss [11]:

$$\sum(V_{oc,n} - V_{oc,rad,n})/n = (kT/q)\ln(\text{ERE}_{ave}), \quad (4)$$

where n is the number of junctions.

The resistance loss of a solar cell is estimated solely from the measured fill factor. Fill factor is dependent upon V_{oc} and ideal fill factor FF_0 , defined as the fill factor without any resistance loss, used in the calculation is empirically expressed by [12],

$$\text{FF}_0 = [v_{oc} - \ln(v_{oc} + 0.72)]/(v_{oc} + 1), \quad (5)$$

where v_{oc} is normalized open-circuit voltage and is given by

$$v_{oc} = V_{oc}/(nkT/q). \quad (6)$$

The measured fill factor FF is decreased as increase in series resistance R_s and decrease in shunt resistance R_{sh} of solar cell and approximated by

$$\text{FF} \approx \text{FF}_0(1 - r_s)(1 - 1/r_{sh}) \approx \text{FF}_0(1 - r_s - 1/r_{sh}), \quad (7)$$

where r_s and r_{sh} are normalized series resistance and normalized shunt resistance, respectively and are given by

$$r_s = R_s/R_{CH} \quad (8)$$

$$r_{sh} = R_{sh}/R_{CH}. \quad (9)$$

The characteristic resistance R_{CH} is expressed by [12]

$$R_{CH} = V_{oc}/I_{sc}. \quad (10)$$

In the calculation, highest values obtained were used as J_{sc} . V_{oc} and FF were calculated by equations (2)–(10) and conversion efficiency potential of various solar cells were calculated as a function of ERE.

4 Analysis for non-radiative recombination loss and efficiency potential of III–V single-junction and multi-junction solar cells

Figure 3 shows calculated efficiencies of GaAs single-junction, III–V 2-junction, III–V/Ge 3-junction and III–V/InGaAs 3-junction solar cells as a function of average external radiative efficiency (ERE) in comparison with the state-of-the-art efficiencies of those solar cells [3] including chronological efficiency improvements [5]. GaAs single-junction, III–V 2-junction and III–V 3-junction solar cells have potential efficiencies of 30%, 37% and 47%, respectively. Highest efficiency of 39.5% [3,13] has been demonstrated with III–V 3-junction solar cells under 1-sun by NREL, further efficiency improvements in III–V multi-junction solar cells by improving ERE and reducing resistance loss are expected. For this end, reduction on non-radiative recombination and resistance losses is necessary.

Figure 4 shows chronological ERE improvements of GaAs single-junction, III–V 2-junction, III–V/Ge 3-junction and III–V/InGaAs 3-junction solar cells.

Although in initial stage of developments, GaAs single-junction and III–V MJ solar cells have shown low ERE values, ERE values have been improved as a result of several technology development. For example, in the case of GaAs single-junction solar cells, hetero-face and double hetero junction solar cells have been developed from homo junction solar cells. Recently, high ERE values have been realized by photon recycling [14,15].

In the case of III–V MJ solar cells, improvements in ERE of sub-cells are necessary for further improvements in efficiencies of MJ solar cells. For example, in the case of 6-junction solar cell [16], ERE ($1.3 \times 10^{-4}\%$) for the 1st 2.19 eV AlGaInP cell 0.044% for the 2nd 1.76 eV AlGaAs cell are lower than 1.4% for the 3rd 1.42 eV GaAs cell and 2.1% for 4th 1.19 eV GaInAs cell and 5th 0.97 eV GaInAs cell. Lower ERE values for Al-related cells are thought to be due to oxygen-related non-radiative recombination center [17].

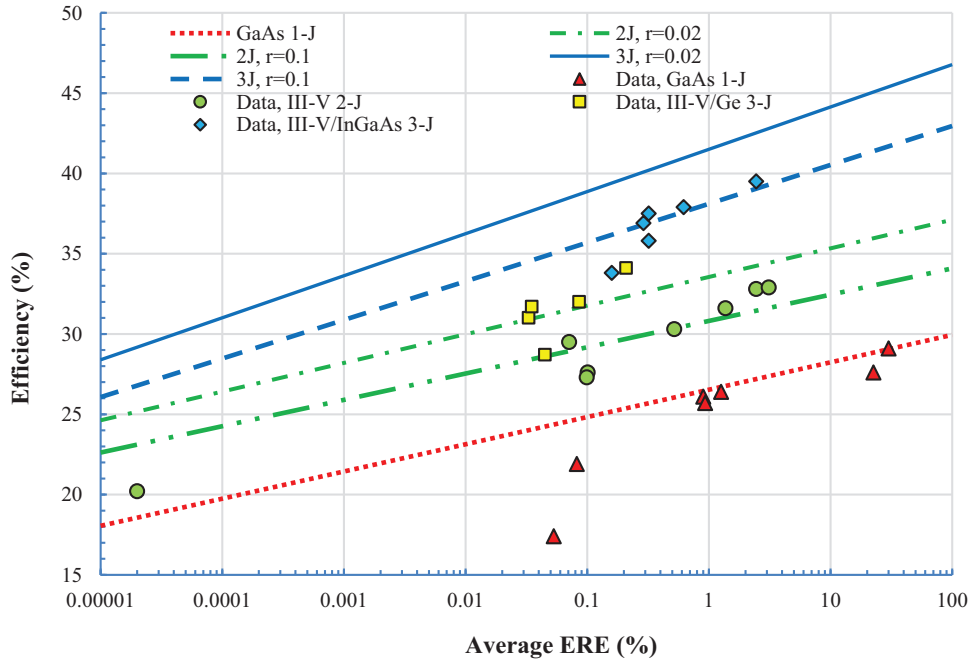


Fig. 3. Calculated efficiencies of GaAs single-junction, III-V 2-junction, III-V/Ge 3-junction and III-V/InGaAs 3-junction solar cells as a function of average ERE in comparison with the state-of-the-art efficiencies of those solar cells including chronological efficiency improvements.

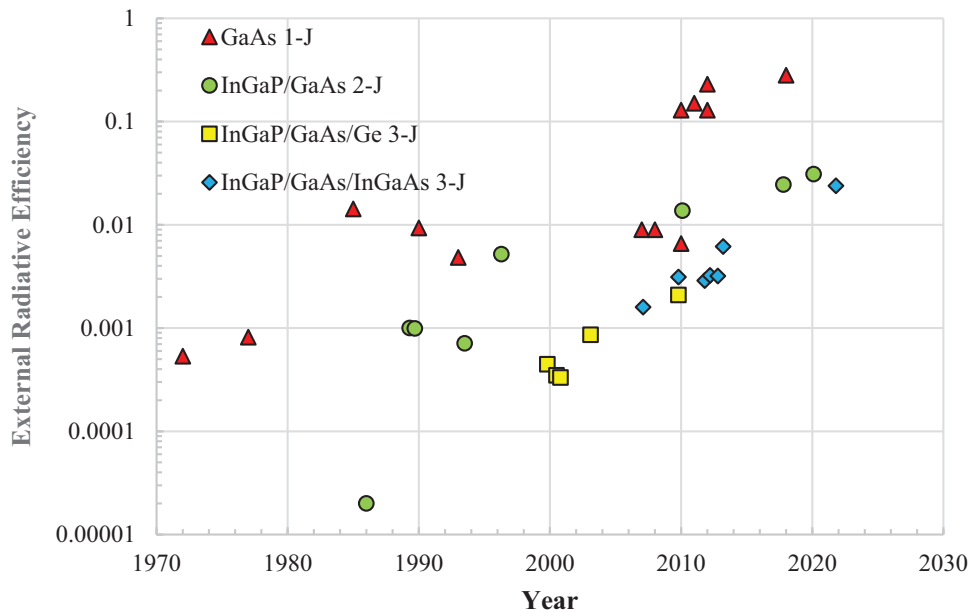


Fig. 4. Chronological ERE improvements of GaAs single-junction, III-V 2-junction, III-V/Ge 3-junction and III-V/InGaAs 3-junction solar cells.

Figure 5 shows chronological fill factor FF improvements of GaAs single-junction, III-V 2-junction, III-V/Ge 3-junction and III-V/InGaAs 3-junction solar cells.

Although in initial stage of developments, GaAs single-junction and III-V MJ solar cells have shown low fill factor values, FF values have been improved as a results of improvements in series resistance and shunt resistance.

Figure 6 shows changes in average external radiative efficiency ERE for III-V multi-junction, III-V/Si tandem solar cells and perovskite/Si tandem solar cells as a function of number of junctions. In Figure 6, estimated average ERE values for GaAs single-junction [3,14], III-V 2-junction [3,18], III-V 3-junction [3,13], III-V 5-junction [3,19], III-V 6-junction [3,16], III-V/Si 2-junction [3,20],

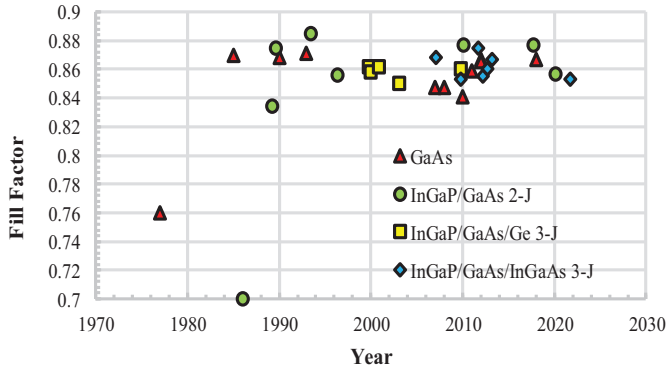


Fig. 5. Chronological fill factor improvements of GaAs single-junction, III-V 2-junction, III-V/Ge 3-junction and III-V/InGaAs 3-junction solar cells.

III-V/Si 3-junction [3,21], perovskite single-junction [3] and perovskite/Si 2-junction [3,22] solar cells were plotted. It is clear in Figure 6 that ERE for III-V MJ and Si tandem solar cells decreases as increase in number of junctions. Further improvements in ERE of sub-cells are necessary for further improvements in efficiencies of MJ and Si tandem solar cells. Especially, in the case of III-V based MJ solar cells, Al contained wide-bandgap sub-cell layer is suggested to be lower ERE due to oxygen-related non-radiative recombination center [17].

In this paper, non-recombination center behavior of AlGaInP top cell and AlGaAs 2nd layer solar cells was analyzed by using data for molecular-beam epitaxy grown $\text{Al}_{0.3}\text{Ga}_{0.7}\text{As}$ solar cells reported by one of the authors [23]. In this analysis, we assumed that the external radiative efficiency IRE is equal to the internal radiative efficiency IRE as follows:

$$\text{ERE} = \text{IRE} = \tau_{\text{eff}}/\tau_{\text{rad}}, \quad (11)$$

where τ_{rad} is the radiative recombination lifetime and expressed by

$$\tau_{\text{rad}} = 1/BN, \quad (12)$$

where N is carrier concentration and B is radiative recombination probability ($2 \times 10^{-10} \text{ cm}^3/\text{s}$ for GaAs [24]).

Effective lifetime τ_{eff} is expressed by

$$1/\tau_{\text{eff}} = 1/\tau_{\text{rad}} + 1/\tau_{\text{nonrad}}, \quad (13)$$

where τ_{nonrad} is non-radiative recombination lifetime and given by

$$1/\tau_{\text{nonrad}} = \sigma v N_r, \quad (14)$$

where σv is minority-carrier thermal velocity, σ is capture cross section of non-radiative recombination centers, and N_r is density of non-radiative recombination centers. In this analysis, 10^{-10} cm^2 was used as capture cross section of oxygen related non-radiative recombination center ($E_c - 0.86 \text{ eV}$ in AlGaAs) by fitting correlation curve between ERE and N_r as shown as dotted line in Figure 7. ERE values were determined by using voltage loss expressed by equation (2).

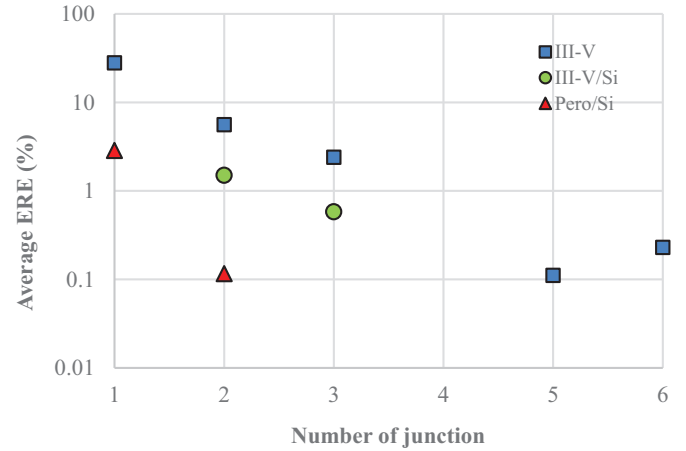


Fig. 6. Changes in average external radiative efficiency ERE for III-V multi-junction, III-V/Si tandem solar cells and perovskite/Si tandem solar cells as a function of number of junctions.

Table 2 shows activation energies and capture cross sections in AlGaAs [25–27] and our result. As shown in Table 2, it is clear that oxygen-related defect in AlGaAs acts as very active defect center because it has higher capture cross section. In addition, the oxygen related defect in AlGaAs has been confirmed to act as a non-radiative recombination center by using double carrier pulse DLTS (Deep Level Transient Spectroscopy) in our previous study [17]. Density of non-recombination center N_r in 2.19 eV AlGaInP top cell and 1.76 eV AlGaAs 2nd layer cell of 6-junction solar cell [16] was estimated by equations (11)–(14) and was compared with data for MBE-grown 1.77 eV AlGaAs single-junction solar cell [23].

Figure 7 shows changes in external radiative efficiency ERE for 2.1 eV AlGaInP top cell and 1.76 eV AlGaAs 2nd layer cell of 6-junction solar cell [16] and MBE-grown 1.77 eV AlGaAs single-junction solar cell [23] as a function of non-radiative recombination centers estimated by using equations (11)–(14). Because ERE ($1.3 \times 10^{-4}\%$) for the 1st 2.19 eV AlGaInP cell 0.044% for the 2nd 1.76 eV AlGaAs cell are lower than 1.4% for the 3rd 1.45 eV (Al)GaAs cell and 2.1% for 4th 1.19 eV GaInAs cell and 5th 0.97 eV GaInAs cell in the 6-junction solar cell [16], reduction in density of non-recombination center in Al-contained wide-bandgap layer is necessary as pointed out by one of co-authors [17]. Lower ERE values for Al-contained solar cells are thought to be due to oxygen-related non-radiative recombination center [17].

Figure 8 shows changes in fill factor FF for III-V multi-junction, III-V/Si tandem solar cells and perovskite/Si tandem solar cells as a function of number of junctions. In Figure 8, reported fill factor values for GaAs single-junction [3,14], III-V 2-junction [3,18], III-V 3-junction [3,22], III-V 5-junction [3,19], III-V 6-junction [3,16], III-V/Si 2-junction [3,20], III-V/Si 3-junction [3,21], perovskite single-junction [3] and perovskite/Si 2-junction [3,22] solar cells were plotted. It is clear in Figure 8 that FF for III-V MJ and Si tandem solar cells decreases as increase

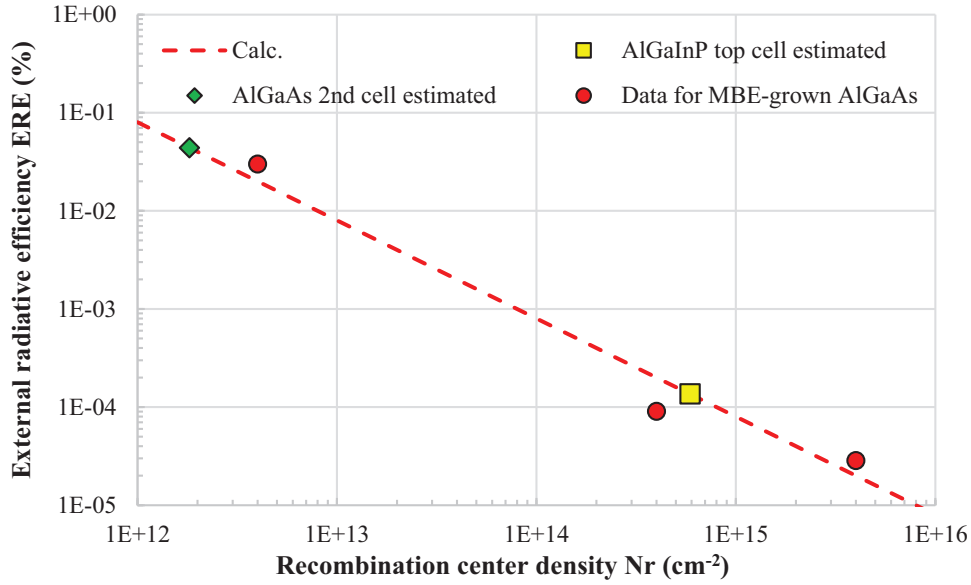


Fig. 7. Changes in external radiative efficiency ERE for AlGaInP top cell and AlGaAs 2nd layer cell of 6-junction solar cell [16] and MBE-grown AlGaAs single-junction solar cell [18] as a function of non-radiative recombination centers estimated by using equations (11)–(14).

Table 2. Activation energies and capture cross sections in AlGaAs [25–27] and our result.

Deep levels	Activation energy (eV)	Capture cross section (cm^2)	Possible origin	References
DX	$E_c - 0.15$ to -0.2	1×10^{-15} to 1×10^{-14}	V_{As} -Donor	[24,26]
A	$E_c - 0.48$	7×10^{-14}	V_{As} - As_i	[27]
B	$E_c - 0.59$	1×10^{-14}		[27]
D	$E_c - 0.81$	3×10^{-13}	Similar defect with EL2 in GaAs	[27]
H	0.4	2×10^{-13}		[27]
Hx	0.56	6×10^{-10}	As-related defect	[27]
PA	$E_c - 0.86$	1×10^{-10}	Oxygen-related defect	This study [17]

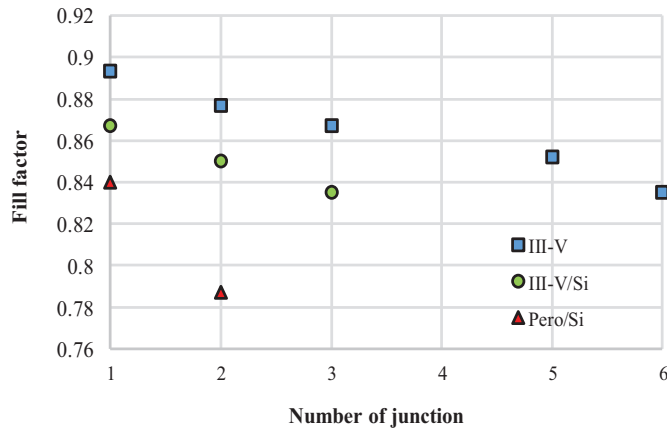


Fig. 8. Changes in fill factor for III–V multi-junction, III–V/Si tandem solar cells and perovskite/Si tandem solar cells as a function of number of junctions.

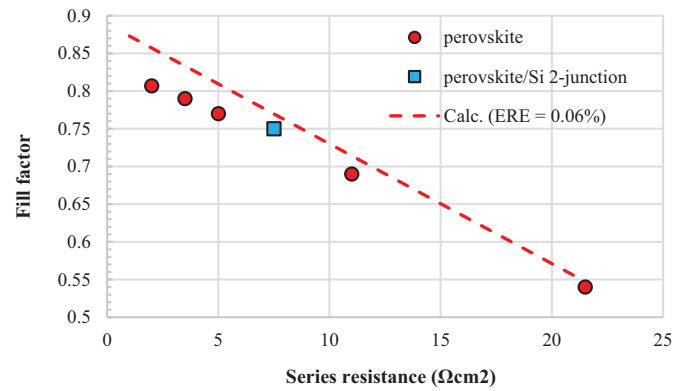


Fig. 9. Correlation between fill factor and contact resistivity of perovskite single-junction and perovskite/Si 2-junction solar cells.

in number of junctions. Further improvements in FF for III–V MJ solar cells and Si tandem solar cells are necessary by improvements in series resistance and shunt resistance.

Although resistance loss is composed of absorber, interface, contact, interconnection and grid of solar cells, especially, fill factor of perovskite/Si tandem solar cells is dependent on contact resistance of interconnection of sub-cells such as transparent conductive oxide layer, recombination junction and so forth. Figure 9 shows correlation between fill factor and series resistance of perovskite single-junction solar cell [28] and perovskite/Si 2-junction solar cell [29]. Calculated results for series resistance of perovskite single-junction solar cell were estimated by using equations (5)–(10). Difference between measured values and calculated results for perovskite single-junction solar cells are thought to be attributed from shunt resistance. Further improvements in FF for perovskite/Si tandem solar cells are necessary by improvements in series resistance and shunt resistance.

5 Summary

This paper overviewed progress in III–V multi-junction (MJ) solar cells. In addition, analytical results for efficiency potential of III–V MJ solar cells were presented and non-radiative recombination and resistance losses of III–V MJ solar cells were discussed in this paper. GaAs single-junction, III–V 2-junction and III–V 3-junction solar cells have potential efficiencies of 30%, 37% and 47%, respectively. Although in initial stage of developments, GaAs single-junction and III–V MJ solar cells have shown low external radiative efficiency ERE values, ERE values have been improved as a result of several technology development such as device structure and material quality developments. It was shown in this study that ERE and fill factor FF for III–V MJ and Si tandem solar cells decreases as increase in number of junctions. Further improvements in FF for III–V MJ solar cells and Si tandem solar cells are necessary by improvements in series resistance and shunt resistance. Improvements in ERE of sub-cells were shown to be necessary for further improvements in efficiencies of MJ solar cells. Especially, Al contained wide-bandgap sub-cell layer showed lower ERE due to oxygen-related non-radiative recombination center.

Conflict of interest

The authors declare no conflict of interest.

Supporting Information

Supporting Information is available from the Wiley Online Library or from the authors.

Data availability

The data that support the findings of this study are available upon reasonable request from the authors.

The authors would like to express sincere thanks to Dr. J.F. Geisz, Dr. M.A. Steiner and Dr. R. France, NREL for their fruitful discussion, to the NEDO for their support and to Dr. T. Takamoto, Sharp, Dr. K. Araki and Dr. K-H. Lee, former Toyota Tech. Inst., Prof. A. Yamamoto, Dr. H. Sugiura, Prof. K. Ando, Dr. C. Amano, Prof. S. Katsumoto and Dr. M. Sugo, Former NTT Labs., Dr. M. Al-Jassim, Dr. R. Ahrienkiel, Dr. J. Olson, Dr. S.R. Kurtz and Dr. D.J. Friedman, NREL, Prof. A. Luque and Prof. G. Sala, UPM, Dr. A. Bett and Dr. G. Siefer, FhG-ISE, Dr. Y. Hishikawa, AIST, Prof. Y. Okada and Prof. M. Sugiyama, Univ. Tokyo, Prof. K. Nishioka and Prof. Y. Ota, Univ. Miyazaki for their helpful discussion and collaboration.

Author contribution statement

The supervision of the project was ensured by M. Yamaguchi. The experiments were conducted by M. Yamaguchi, N. Ekins-Daukes and N. Kojima. The analysis was conducted by M. Yamaguchi, F. Dimroth and N. Ohshita. Discussion on results was conducted by all co-authors. The writing of the manuscript and proof reading were done by all co-authors.

References

1. W. Shockley, H.J. Queisser, Detailed balance limit of efficiency of p-n Junction solar cells, *J. Appl. Phys.* **32**, 510 (1961)
2. M. Yamaguchi, F. Dimroth, J.F. Geisz, N.J. Ekins-Daukes, Multi-junction solar cells paving the way for super high-efficiency, *J. Appl. Phys.* **129**, 240901 (2021)
3. M.A. Green, E.D. Dunlop, J. Hohl-Ebinger, M. Yoshita, N. Kopidakis, K. Bothe, D. Hinken, M. Rauer, X. Hao, Solar cell efficiency tables (version 60), *Prog. Photovolt.* **30**, 687 (2022)
4. A. Goetzberger, J. Luther, G. Willeke, Solar cells: past, present, future, *Solar Energy Mater. Solar Cells* **74**, 1 (2002)
5. M. Yamaguchi, K-H. Lee, K. Araki, N. Kojima, A review of recent progress in heterogeneous silicon tandem solar cells, *J. Phys. D: Appl. Phys.* **51**, 133002 (2018)
6. U. Rau, Reciprocity relation between photovoltaic quantum efficiency and electroluminescent emission of solar cells, *Phys. Rev. B* **76**, 085303 (2007)
7. M.A. Green, Radiative efficiency of state-of-the-art photovoltaic cells, *Prog. Photovolt.* **20**, 472 (2012)
8. J. Yao, T. Kirchartz, M.S. Vezie, M.A. Faist, W. Gong, Z. He, H. Wu, J. Troughton, T. Watson, D. Bryant, J. Nelson, Quantifying losses in open-circuit voltage in solution-processable solar cells, *J. Phys. Rev. Appl.* **4**, 014020 (2015)
9. M. Yamaguchi, H. Yamada, Y. Katsumata, K-H. Lee, K. Araki, N. Kojima, Efficiency potential and recent activities of high-efficiency solar cells, *J. Mater. Res.* **32**, 3446 (2017)
10. M. Yamaguchi, K.H. Lee, K. Araki, N. Kojima, H. Yamada, Y. Katsumata, Analysis for efficiency potential of high-efficiency and next generation solar cells, *Prog. Photovolt.* **26**, 543 (2018)
11. M. Yamaguchi, K-H. Lee, P. Schygulla, F. Dimroth, T. Takamoto, R. Ozaki, K. Nakamura, N. Kojima, Y. Ohshita, Approaches for high-efficiency III-V/Si tandem solar cells, *Energy Power Eng.* **13**, 413 (2021)
12. M.A. Green, *Solar Cells* (UNSW, Kensington, 1998), p. 96
13. R.M. France, J.F. Geisz, T. Song, W. Olavarria, M. Young, A. Kibbler, M.A. Steiner, Triple-junction solar cells with

- 39.5% terrestrial and 34.2% space efficiency enabled by thick quantum well superlattices, *Joule* **6**, 1121 (2022)
14. B.M. Kayes, H. Nie, R. Twist, S.G. Spruytte, F. Reinhardt, I.C. Kizilyalli, G.S. Higashi, 27.6% conversion efficiency: a new record for single-junction solar cells under 1 sun illumination, in *Proceedings of the 37th IEEE Photovoltaic Conference* (IEEE, New York, 2011), p. 4
 15. J.F. Geisz, M.A. Steiner, I. García, S.R. Kurtz, D.J. Friedman, Enhanced external radiative efficiency for 20.8% efficient single-junction GaInP solar cells, *Appl. Phys. Lett.* **103**, 041118 (2013)
 16. J.F. Geisz, R.M. France, K.L. Schulte, M.A. Steiner, A.G. Norman, H.L. Guthrey, M.R. Young, T. Song, T. Moriarty, Six-junction III-V solar cells with 47.1% conversion efficiency under 143 suns concentration, *Nat. Energy* **5**, 326 (2020)
 17. K. Ando, C. Amano, H. Sugiura, M. Yamaguchi, A. Saletes, Nonradiative e-h recombination characteristics of mid-gap electron trap in $\text{Al}_x\text{Ga}_{1-x}\text{As}$ ($x=0.4$) grown by MBE, *Jpn J. Appl. Phys.* **26**, L266 (1987)
 18. M.A. Steiner, R.M. France, J. Buencuerpo, J.F. Geisz, M.P. Nielsen, A. Pusch, W.J. Olavarria, M. Young, N.J. Ekins-Daukes, High efficiency inverted GaAs and GaInP/GaAs solar cells with strain-balanced GaInAs/GaAsP quantum wells, *Adv. Energy Mater.* **11**, 2002874 (2021)
 19. P.T. Chiu, D.C. Law, R.L. Woo, S.B. Singer, D. Bhusari, W.D. Hong, A. Zakaria, J. Boisvert, S. Mesropian, R.R. King, N.H. Karam, 35.8% space and 38.8% terrestrial 5J direct bonded cells, in *Proceedings of the 40th IEEE Photovoltaic Specialist Conference* (IEEE, New York, 2014), pp.0011–0013
 20. S. Essig, C. Allebe, T. Remo, J.F. Geisz, M.A. Steiner, K. Horowitz, L. Barraud, J.S. Ward, M. Schnabel, A. Descoedres, D.L. Young, M. Woodhouse, M. Despeisse, C. Ballif, A. Tamboil, Raising the one-sun conversion efficiency of III-V/Si solar cells to 32.8% for two junctions and 35.9% for three junctions, *Nat. Energy* **2**, 17144 (2017)
 21. P. Schygulla, R. Müller, D. Lackner, O. Höhn, H. Hauser, B. Bläsi, F. Predan, J. Benick, M. Hermle, S.W. Glunz, F. Dimroth, Two-terminal III-V//Si triple-junction solar cell with power conversion efficiency of 35.9% atAM1.5g, *Prog. Photovolt.* **30**, 869 (2022)
 22. P. Tockhorn, J. Sutter, A. Cruz, P. Wagner, K. Jäger, D. Yoo, F. Lang, M. Grischek, B. Li, A. Al-Ashouri, E. Köhnen, M. Stolterfoht, D. Neher, R. Schlatmann, B. Rech, B. Stannowski, S. Albrecht, C. Becker, Nano-optical designs enhance monolithic perovskite/silicon tandem solar cells toward 29.8% efficiency, *Res. Square*, <https://doi.org/10.21203/rs.3.rs-1439562/v1>
 23. C. Amano, H. Sugiura, K. Ando, M. Yamaguchi, High-efficiency $\text{Al}_{0.3}\text{Ga}_{0.7}\text{As}$ solar cells grown by molecular beam epitaxy, *Appl. Phys. Lett.* **51**, 1075 (1987)
 24. K. Sasaki, T. Agui, K. Nakaido, N. Takahashi, R. Onitsuka, T. Takamoto, Development of InGaP/GaAs/InGaAs inverted triple junction concentrator solar cells, *AIP Conf. Proc.* **1556**, 22 (2013)
 25. D.V. Lang, R.A. Logan, M. Jaros, Trapping characteristics and a donor-complex (DX) model for the persistent-photoconductivity trapping center in Te-doped $\text{Al}_x\text{Ga}_{1-x}\text{As}$, *Phys. Rev. B* **19**, 1015 (1979)
 26. P.M. Mooney, Deep donor levels (DX centers) in III-V semiconductors, *J. Appl. Phys.* **67**, R1 (1990)
 27. A. Cavallini, B. Fraboni, F. Capotondi, L. Sorba, G. Biasiol, Deep levels in MBE grown AlGaAs/GaAs heterostructures, *Microelectr. Eng.* **73–74**, 954 (2004)
 28. N. Mundhaas, Z.J. Yu, K.A. Bush, H-P. Wang, J. Häusele, S. Kavadiya, M.D. McGehee, Z.C. Holman, Series resistance measurements of perovskite solar cells using $J_{sc} - V_{oc}$ measurements, *Solar RRL* **3**, 1800378 (2019)
 29. C. McDonald, H. Sai, V. Svrcek, A. Kogo, T. Miyadera, T.N. Murakami, M. Chikamatsu, Y. Yoshida, T. Matsui, In situ grown nanocrystalline Si recombination junction layers for efficient perovskite–Si monolithic tandem solar cells: Toward a simpler multijunction architecture, *ACS Appl. Mater. Interfaces* **14**, 33505 (2022)

Cite this article as: Masafumi Yamaguchi, Frank Dimroth, Nicholas J. Ekins-Daukes, Nobuaki Kojima, Yoshio Ohshita, Overview and loss analysis of III–V single-junction and multi-junction solar cells, *EPJ Photovoltaics* **13**, 22 (2022)